Advances in Aerodynamics

RESEARCH

Open Access

Effect of vortex generator spanwise height distribution pattern on aerodynamic characteristics of a straight wing

Lishu Hao[1*], Bao Hu[1], Yongwei Gao[1] and Binbin Wei[2]

*Correspondence:
haolishu@nwpu.edu.cn

[1] School of Aeronautics, Northwestern Polytechnical University, Xi'an 710072, China
[2] School of Aerospace Engineering, Xi'an Jiaotong University, Xi'an 710049, China

Abstract

Vortex generator (VG) is a passive flow control technology, which can effectively inhibit flow separation. Recently, significant research efforts have been devoted to the study on the application of VG in airfoil, wing/blade and aircraft flow separation inhibition. However, the research on the variable height distribution of VG along the wingspan still lacks. This study focuses on the experimental investigation of the influence of variable height distribution of ramp VG on aerodynamic characteristics. First, VG was designed, such that it was composed of two parts, one fixed region and one deformed region, which allowed for height modification. The height of VGs along the wingspan presented equal-height, triangular and trapezoidal distribution, forming a total of 15 VG layouts. Then, the connection mode of the model, the change of angle of attack and the collection and processing of aerodynamic data were introduced. Finally, a wind tunnel experiment was performed to investigate the influence of height distribution of VG on aerodynamic characteristics of wing. The experimental results show that: (1) the height distribution of the three types of VGs could inhibit the stall flow and improve the aerodynamic performance of the wing; (2) "Triangular translation 3" and "Trapezoidal translation 2" were the best layouts, both of which could increase the maximum lift coefficient, delay stall, and significantly increase the lift-to-drag ratio at high angle of attack; (3) the influence of VG height and position factors on wing stall characteristics was analyzed by using the rough set theory, and the key position information of VG arrangement was provided. This study indicates that the variable height distribution is obviously better than the equal height distribution, which can provide ideas and references for the active control of variable height distribution of VGs.

Keywords: Vortex generator, Flow control, Rough set theory, Wind tunnel experiment

1 Introduction

The concept of vortex generator (VG) was first proposed by Taylor in 1947 [1], to realize the energy exchange between the low and high energy zone of the boundary layer, and to enhance lift and reduce drag at the wing of an aircraft. Traditionally, it is a passive flow control technology, and is the most popular choice for modern large-scale horizontal axis wind turbines. The shape of VGs can be divided into vane-type, ramp-type and wishbone [2]. Fernandez-Gamiz et al. [3] carried out the test of self-similarity

and helical symmetry in VG flow simulations. At present, VGs are widely used for flow control of airfoils [4, 5], wind turbine blades [6–8], inlets [9–11], etc., and they are also economical [12].

The flow control on static airfoils finds application prospects in fixed-wing aircrafts such as transport and fighter aircrafts; thus, numerous flow control techniques have been studied. To date, forty-one different triangular vane-type VGs have been designed to study their effect on aerodynamic characteristics of airfoils [13]. The results showed that the chordwise position, vane height, and array configuration are the main effective factors; and the vane length, inclination angle, shape, and array packing density are the secondary effective factors. Zhang et al. [14] applied triangular vane-type VGs to wind turbine airfoils with three different thicknesses and realized effective stall control. Kim et al. [15] proposed a variable-incidence-angle triangular vane-type VG and applied it to realize the stall control over an NACA0015 airfoil. Further, Wang et al. [16] applied rectangular vane-type VGs to control the stall of an S809 airfoil, and studied the effects of length and layout position of VG on aerodynamic characteristics of the airfoil. Arunvinthan [17] and Zhang et al. [18] carried out bionic design regarding the shape of VGs and carried out beneficial studies and practices on the control of airfoil stalls.

Dynamic stall control on dynamic airfoils has also been studied in order to achieve flow control for typical unsteady conditions, such as for helicopters and wind turbines. For instance, Zhu et al. [19] applied rectangular vane-type VGs to control the dynamic stall of an S809 airfoil and achieved effective dynamic stall control. Zhu et al. [20] applied triangular vane-type VGs to control the dynamic stall of a DU-97-W300 airfoil and studied the effect of VG height and chordwise position on the unsteady aerodynamic response. De Tavernier et al. [21] applied triangular vane-type VGs to the dynamic stall control of wind turbine blade airfoils, thus confirming that the mounting location and height of VG played key roles. Le Pape et al. [22] designed a row of deployable VGs and addressed the validation of the effectiveness of VGs to delay static stall and alleviate dynamic stall.

Practically, VGs with three-dimensional flow control are widely used in wind turbine blades. For instance, Moon et al. [7] arranged trapezoidal vane-type VGs in the inboard sections of wind turbine blade. Consequently, the effects of chordwise length, height, and interval of the fair of VGs on aerodynamic characteristics of the wind turbine blade were studied. Lee et al. [8] arranged triangular vane-type VGs in the inboard region of an NREL 5 MW wind turbine blade and were able to achieve an effective control effect of the separation flow on the blade. Troldborg et al. [23] adopted numerical simulation for the DTU 10 MW wind turbine blade with triangular vane-type VGs, and studied the effect of the installation position of the VG along the wingspan direction of the blade. Wu et al. [24] carried out numerical simulation on rectangular vane-type VGs for the blade root of a WindPACT 1.5 MW wind turbine and studied the development and evolution of separate vortices near the VG.

Currently, the study on flow control for boundary layers using VGs focuses on their shape, installation position, height, spacing, and number. In particular, for the control of three-dimensional separation flow such as on the wing/blade, a series of VGs with equal height is arranged; however, this is not conducive to the control of separation vortices derived from the chordwise and spanwise direction. Therefore, the effect of

height variation of a VG along the wingspan direction on the aerodynamic characteristics of a wing was studied herein.

The structure of this paper is organized into four sections. First, the "Introduction" section (Section 1) discusses the original objective of the research. Then, the ramp VG design and experiment device in wind tunnel test is introduced in the "Experiment and procedure" section (Section 2). The "Results and discussion" section (Section 3) mainly presents the analysis of the influence of various layout forms of VG on the aerodynamic characteristics of the model, and further provides the exploration of the comprehensive reasons through the rough set theory. Finally, in the "Conclusion" section (Section 4), the research of this paper is summarized and further outlook is presented.

2 Experiment and procedure

2.1 Wind tunnel experiment

The experiment was carried out in a DC open wind tunnel of Northwestern Polytechnical University, and the wind speed in the experiment was 20 $m \cdot s^{-1}$.

The experimental model consisted of a straight wing with an NACA4415 airfoil. The interior of the model was composed of a steel wood mixed structure, which consisted of a wooden filling. The chordwise and spanwise lengths of the model were 400 and 800 mm, respectively. The model installation and wind tunnel structure are shown in Fig. 1. In the wind tunnel anechoic chamber, the bottom is implemented with the angle of attack mechanism, which can not only change the angle of attack of the model, but also realize the support to the model. Between the angle of attack mechanism and the model from top to bottom are the conformal segment model and the balance device. During the experiment, the variation range of the angle of attack is -6° to 28°, and when it is above 16°, the interval changes from two to one degree.

A six-component balance was used to measure the force and pitching moment of the model. The scale of the balance is presented in Table 1. An NI acquisition system was used to acquire the balance signals. The data acquisition frequency was 10 kHz, the system cut-off frequency was 20 kHz, and the sampling time was 10 s, thus the final output voltage signal was the average value of 10^5 data in a measurement process. The aerodynamic coefficient of the body axes was obtained by processing the data using the balance calibration formula. Then, the conversion formula between the

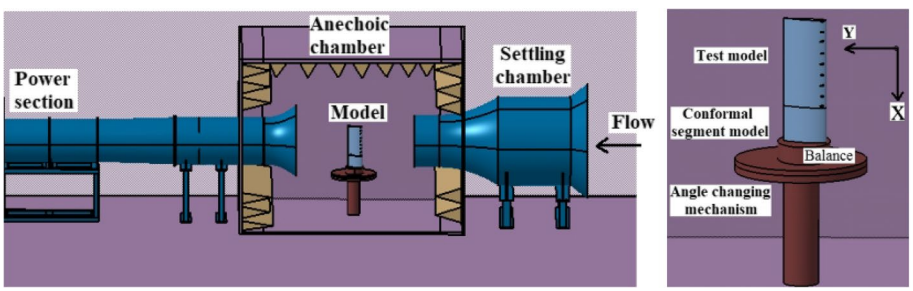

Fig. 1 Schematic of wind tunnel structure and model installation

Table 1 Measurement range and calibration results of the balance

Item	Y	Mz	X	Mx	Z	My
Design load (N, N·m)	1200	200	600	100	150	100
Calibration load (N, N·m)	1200	120	400	40	300	30
Absolute error (N, N·m)	2.4	0.24	0.8	0.08	0.6	0.06
Accuracy (%)	0.2	0.2	0.2	0.2	0.2	0.2
Precision (%)	0.02	0.02	0.02	0.06	0.02	0.02

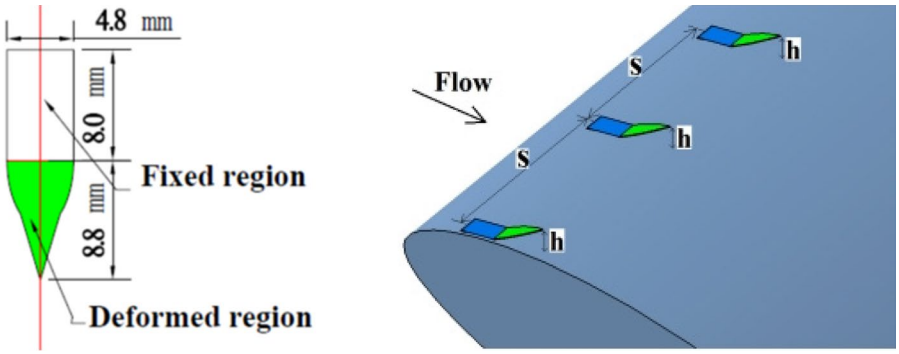

(a) Schematic illustration (b) Layout

Fig. 2 Schematic illustration and layout of ramp-type VG

body axes and the wind axes was used to finally obtain the lift coefficient and drag coefficient of the model for plotting.

2.2 VG configuration

A height-adjustable thin sheet VG, in accordance with the structural characteristics of the ramp-type VG, was designed in this study, as shown in Fig. 2. The VG with a thickness of 0.5 mm was made of titanium-nickel. It consisted of two parts, a fixed region and a deformed region, which enabled height modifications. The fixed region was rectangular in shape and it was used for fixing on the model surface, while the deformed region was similar to a triangle for changing the height of the VG. The VGs were placed at 10%c away from the leading edge, as shown in Fig. 2.

In this study, the variation of VG height along the wing span direction was studied, where the VG was considered according to three height distributions, i.e., equal height, triangular shape, and trapezoidal shape.

In the first experiment, the VG height presents an equal height distribution, as shown in Fig. 3. Herein, the ratio of VG height to chord length is 0.01125. Further, the change of VG layout density is discussed herein, i.e., the number of VGs is 5, 9, 17, and 33, denoted as "Equal height 5", "Equal height 9", "Equal height 17", and "Equal height 33", respectively. The x-axis shown in Fig. 3 represents the installation position of the VGs in the spanwise direction, the y-axis represents the number of VGs, and the coordinate origin is located on the symmetric section of the model.

In the second experiment, the VG height presents a triangular shape distribution, as shown in Fig. 4. The installation position of the VG was the same as for "Equal

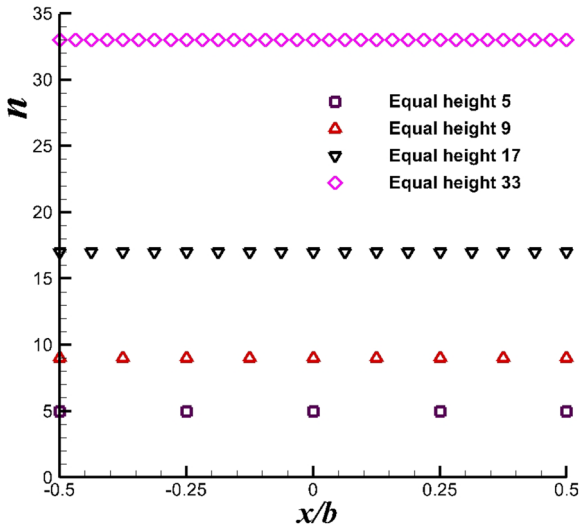

Fig. 3 VG height with equal height distribution

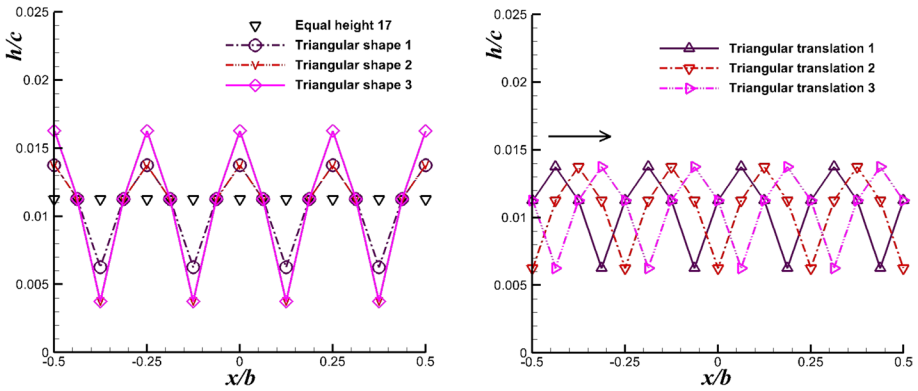

Fig. 4 VG height with triangular shape distribution

height 17". Based on "Triangular shape 1", the VG height of the lowest point could be lowered to form "Triangular shape 2", and then the VG height of the highest point could be increased to form "Triangular shape 3" based on "Triangular shape 2". Next, the shape of "Triangular shape 1" was kept unchanged and then moved from left to right in turn by changing the height of the VG to form "Triangular translation 1", "Triangular translation 2" and "Triangular translation 3", respectively.

In the third experiment, the VG height presents a trapezoidal shape distribution, as shown in Fig. 5. The installation position of the VG was the same as for "Equal height 17". Based on "Trapezoidal shape 1", the VG height of the highest point could be increased to form "Trapezoidal shape 2". Next, the shape of "Trapezoidal shape 1" was kept unchanged and then moved from left to right in turn by changing the height of the VG to form "Trapezoidal translation 1", "Trapezoidal translation 2" and "Trapezoidal translation 3", respectively.

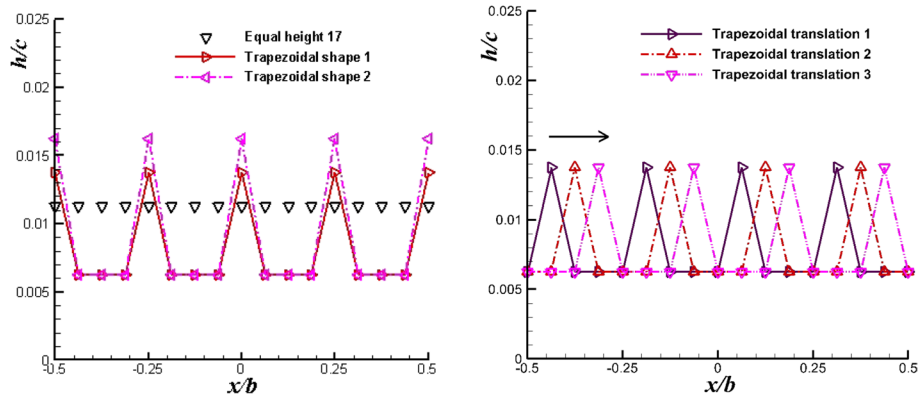

Fig. 5 VG height with trapezoidal shape distribution

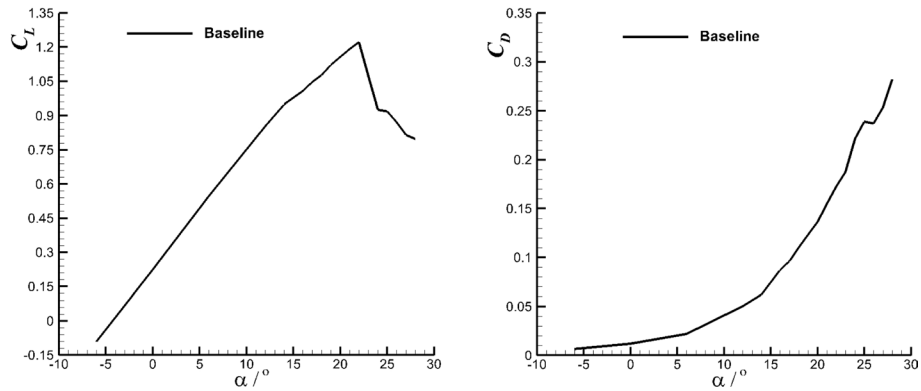

(a) Lift coefficient (b) Drag coefficient

Fig. 6 Variations of the aerodynamic coefficient curves of wing

3 Results and discussion

In this section, the effects of parameters including the equal height, triangular distribution, and trapezoidal distribution of VG height on the static aerodynamic characteristics of the wing are discussed, and analysis of the effect of height variation area on flow control effect is also presented.

3.1 Clean wing

The clean wing without VGs is denoted as "Baseline".

The objective of this study was to use VGs to improve the stall characteristics of a straight wing, and thus it was necessary to obtain the flow separation information about the wing. Figure 6 shows the variations of the aerodynamic coefficient curves of the wing. The stall α was 22°, and the maximum lift coefficient, C_L, was 1.221. When α was greater than stall α, C_L decreased sharply, and then α remained approximately constant for a bit between 24° and 25°. Following this, the separation area continued to expand with the increase of α, resulting in a further decrease of C_L and a continued increase in drag coefficient C_D.

Unfortunately, only the aerodynamic force in the experimental model was obtained in this experiment, and the surface pressure information of the model was not obtained.

Considering that the airfoil used in this study was trailing edge separation, the Kirchhoff flow theory [25] was used to analyze separation position. A special case of this theory involves the simplification of the trailing edge separation phenomenon through a simple model, as indicated by using the following equation:

$$C_n(\alpha) = k(\alpha - \alpha_0)\left(\frac{1+\sqrt{f(\alpha)}}{2}\right)^2, \tag{1}$$

where, k is the slope of the normal force line, α_0 is the zero-lift α, C_n is the normal force coefficient, and f is the position of the separation point. For the reference wing (Baseline), the separation point was calculated by using Eq. 1 as shown in Fig. 7.

The figure shows that the flow separation position at the stall α was $x/c \approx 0.78$, and the flow separation point position was 0.33 when α was 25°.

Previous studies showed that the ramp-type VG should be placed at 5–15%c [26, 27], while the other related literature [28] further suggested that the VG should be placed at 8%c for the NACA4415 straight wing. Therefore, in this study, the VG was placed at 10%c away from the leading edge, and the end point of the VG was approximately at 17%c, which made it possible to control the separated flow occurring at angle below α of 25°.

3.2 Equal height distribution

Figure 8 shows the variations of the aerodynamic coefficient curves of the wing with different numbers of VG. The figure indicates that: (1) When α was small, VG led to the decrease in the C_L of the wing. This is attributed to the fact that the VG was too close to the wing leading edge, which disturbed and destroyed the attached flow on the wing. The more the number of VGs, the stronger the destroying effect, and the more obvious the drop of C_L. However, when the VG number was increased from 17 to 33, the drop in lift coefficient was very limited. (2) When α was large, the stall characteristics of the wing improved, the stall α increased, and the maximum C_L decreased. However, the C_L values for "Equal height 9", "Equal height 17", and "Equal height 33" were obviously better

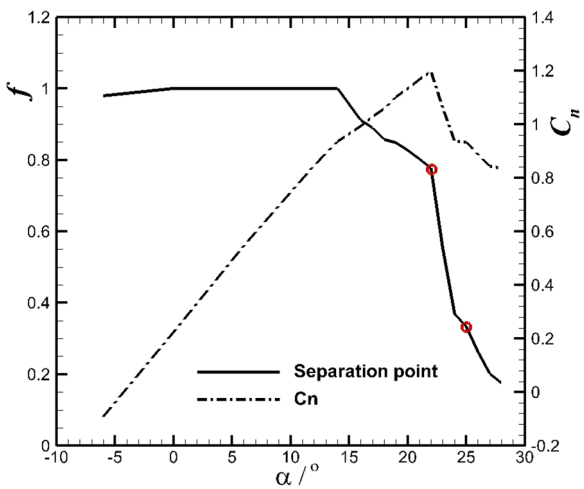

Fig. 7 Normal force coefficient and separation point of reference wing

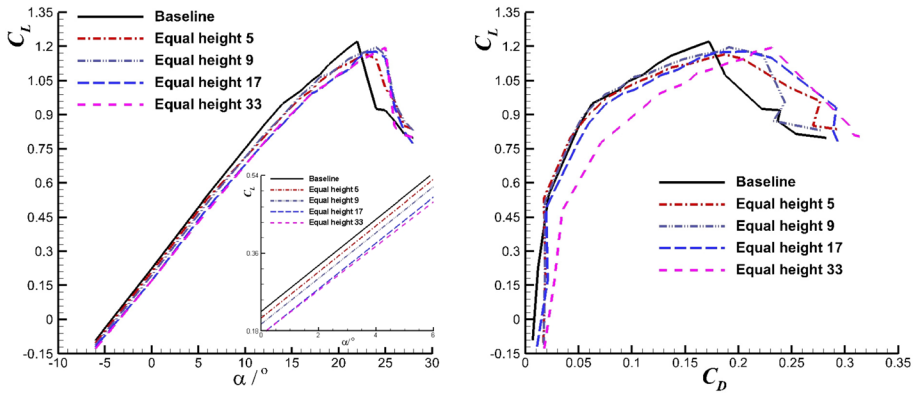

(a) Lift coefficient (b) Drag polar curve

Fig. 8 Variations of the aerodynamic coefficient curves for the wing with different VG numbers

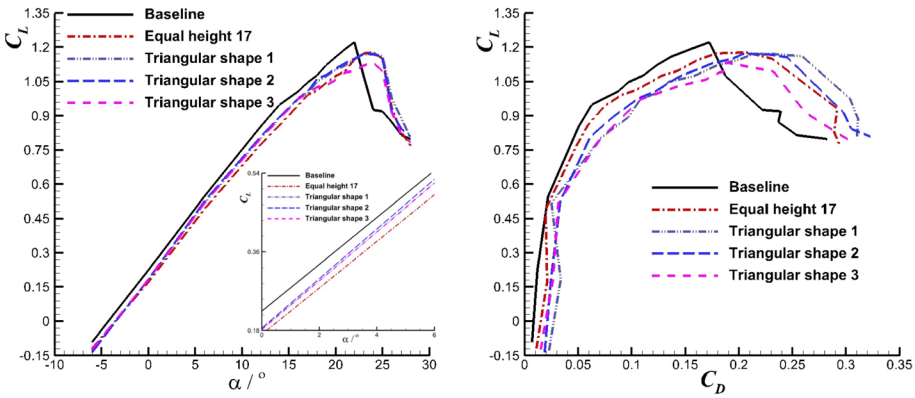

(a) Lift coefficient (b) Drag polar curve

Fig. 9 Variations of the aerodynamic coefficient curves for the wing with different triangular shapes

than that for "Equal height 5". (3) When α was beyond 22°, the lift-to-drag ratio of the wing improved significantly for the VGs with four different density distributions, and "Equal height 17" was the best for improving the lift-to-drag ratio and lift. Therefore, the number of VGs was fixed at 17 in subsequent experiments on the change of VG height along the spanwise direction.

3.3 Triangular distribution

Figure 9 shows the variations of the aerodynamic coefficient curves of the wing when the VG height on the wing presents different triangular shapes. The figure illustrates that: (1) When the α was small, VG led to the decrease in the C_L of the wing, and the amplitude of the reduction was smaller than that of the VG with equal height distribution. This is attributed to the fact that the lowest height in the triangular shape distribution led to reduced destruction of the attached flow on the wing. (2) When the α was high, the stall characteristics of the wing improved, the stall α increased, and all the maximum lift coefficients decreased. The lift coefficients of "Equal height 17", "Triangular shape 1",

and "Triangular shape 2" were higher than those of "Triangular shape 3" in the range of α improved by stall characteristics. This is because the highest point of "Triangular shape 3" was too high, as a result, it was not conducive for the VG to supply energy to the low energy region of the boundary layer. (3) When the α was above 22°, the lift-to-drag ratio of the wing improved significantly for the four different VGs; and "Triangular shape 1" and "Triangular shape 2" were better than "Equal height 17" for the improvement of lift-to-drag ratio. Among the four different VGs, "Triangular shape 3" was the weakest in terms of lift-drag ratio and lift improvement ability, while "Triangular shape 1" was the best. Therefore, VG height distribution of "Triangular shape 1" was subsequently translated along the wing spanwise direction to systematically explore the influence on wing stall flow.

Figure 10 shows the variations of the aerodynamic coefficient curves for the wing when the height distribution of VGs on the wing was triangular and shifted in the spanwise direction. The figure demonstrates that: (1) When the α was low, the VG led to the decrease in the lift coefficient of the wing. In terms of the reduction amplitude, the "Triangular shape 1" after translation was smaller than that before translation, and the reduction amplitude of "Triangular shape 1" was the largest. This is attributed to the fact that the wing surface was dominated by the attached flow at small angles of attack. The height of VG with "Triangular shape 1" in the wing tip zone reduced after translation, and the disturbance to the boundary layer was reduced accordingly. Moreover, the degree of lift reduction was expected to weaken accordingly. (2) When the α was high, the stall characteristics of the wing improved, the stall α increased, and the maximum lift coefficient also increased. The "Triangular translation 3" was the best, the maximum lift coefficient increased by 2.5%, the stall α increased by 2°, and the effective range of α to improve the stall was more than 8°. (3) In the range of α improved by stall characteristics, an increase in lift-to-drag ratio of wing was achieved both before and after the "Triangular shape 1" translation, and "Triangular translation 3" exhibited the best ability to improve lift-drag-ratio and lift among all before and after triangular height distribution translation plan. Therefore, the height change of VGs near the wing tip significantly impacts the improvement of wing stall characteristics, which in turn affects the

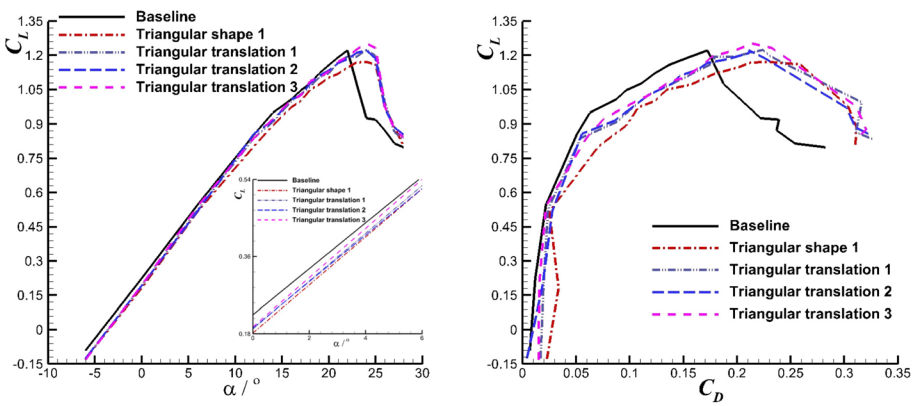

(a) Lift coefficient (b) Drag polar curve

Fig. 10 Variations of the aerodynamic coefficient curves for the wing with different triangular translations

development of the wing tip vortex, i.e., the height change of VGs at the wing tip is a key factor for controlling stall flow of the wing.

3.4 Trapezoidal distribution

Figure 11 shows the variations of the aerodynamic coefficient curves of the wing when the VG height on the wing presents different trapezoidal shapes. The figure reveals that: (1) When the α was low, VG led to the decrease in the lift coefficient of the wing. The trapezoidal shape showed smaller values for the reduction amplitude compared to those for equal height, and those for "Trapezoidal shape 1" were the smallest. This is attributed to the fact that the lowest height in the trapezoidal shape distribution reduced the damage to the attached flow on the wing. (2) When the α was high, the stall characteristics of the wing improved, the stall α increased, and all the maximum lift coefficients decreased. In the range of α improved by stall characteristics, the VG height distribution with equal height 17 and trapezoidal shape shows similar suppression ability to wing separation flow. (3) From the aspect of lift-drag-ratio, the VG height with trapezoidal distribution at high α showed better ability to improve lift-drag-ratio than the equal height distribution. Therefore, herein, subsequent research was carried out on the height distribution translation change of the VG in "Trapezoidal shape 1".

Figure 12 shows the variations of the aerodynamic coefficient curves of the wing when the height distribution of VG on the wing was trapezoidal and shifted in the spanwise direction. The figure presents that: (1) When the α was low, the VG led to the decrease in the lift coefficient of the wing. In terms of the reduction amplitudes, the "Trapezoidal translation 1" showed the smallest values. With the increase in the α, the decrease in the lift coefficient lessened. This is because the VG does not excessively damage the flow around the wing when it presents a trapezoidal shape height distribution. (2) When the α was high, the stall characteristics of the wing improved, the stall α increased, and the maximum lift coefficient also increased. The maximum lift coefficient of "Trapezoidal translation 2" increased by 1.7%, the stall α increased by 2°, and the effective range of α to improve stall was more than 8°. (3) In the range of α improved by stall characteristics, an increase in lift-to-drag ratio of wing was achieved both before and after the "Trapezoidal shape 1" translation, and "Trapezoidal translation 2" showed the best ability to

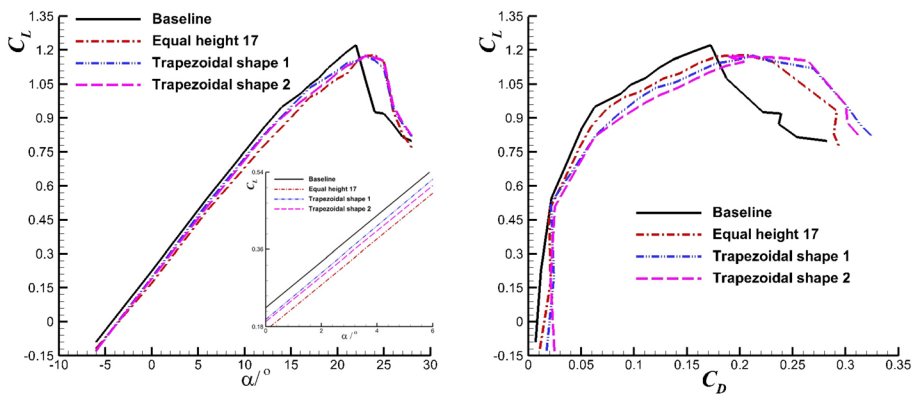

(a) Lift coefficient (b) Drag polar curve

Fig. 11 Variations of the aerodynamic coefficient curves for the wing with different trapezoidal shapes

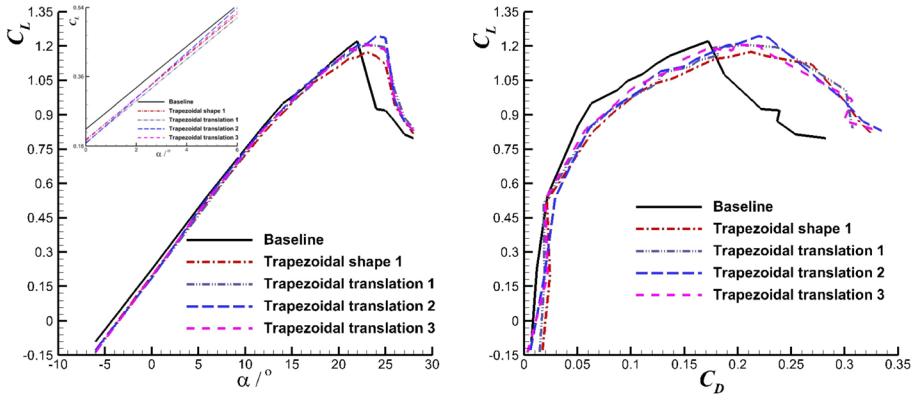

(a) Lift coefficient (b) Drag polar curve

Fig. 12 Variations of the aerodynamic coefficient curves for the wing with different trapezoidal translations

improve lift-drag-ratio and lift among the four different VGs. Specifically, the height of the third installation position was the highest from the wing tip. In the translation of the triangular height shape distribution, the optimal translation was "Triangular translation 3", i.e., the height of the fourth installation position was the highest from the wing tip. Therefore, the height variation of the VG in the wing tip region significantly impacts the improvement of wing stall characteristics.

The VG height distribution in the wing tip zone could affect the VG suppression of the wing stall flow. Therefore, the variation of VG height in the wing tip region significantly influenced the improvement of wing stall characteristics. Next, rough set theory was used to analyze and provide the specific location of VG in the wing tip area.

3.5 Rough set theory analysis

Herein, rough set theory [29] was used for an in-depth analysis of the experimental results. Rough set theory is a typical data mining technology. The basic idea is to summarize concepts and rules through the classification of case bases, and to analyze and process existing data samples. Moreover, it does not need prior knowledge and is highly objective. Related concepts and algorithms of rough set theory are given in literature studies [30, 31] and thus not described herein.

A lot of experimental data were generated in the process of studying the control effect of different VG height distributions on the wing. For the control effect of VG, this study focused on the increase of maximum C_L and stall α. Therefore, the maximum C_L and stall α were selected as the decision attributes in the rough set analysis, and VG heights at different spanwise positions were considered as the conditional attributes. Herein, the experimental results of 17 VGs were selected for analysis, and "clear wing" was regarded as the case where the VG height was 0, for comparative analysis. Therefore, there were 17 conditional attributes and a total of 13 sample cases. The original decision information is presented in Table 2, which was discretized by using the dynamic hierarchical clustering algorithm [31], and the corresponding results are summarized in Table 3.

The maximum C_L was taken as the decision attribute for analysis, and only C_1 (x/c = -0.5), C_2 (x/c = -0.4375), and C_3 (x/c = -0.375) were retained after attribute

Table 2 The original decision information table

No	C_1 $x/c=$-0.5	C_2 -0.4375	C_3 -0.375	....	C_{15} 0.375	C_{16} 0.4375	C_{17} 0.5	D_1 C_{Lmax}	D_2 Stall α
1	0	0	0	.....	0	0	0	1.221	22
2	0.0225	0.0225	0.0225	.....	0.0225	0.0225	0.0225	1.178	24
3	0.0275	0.0225	0.0125	.....	0.0125	0.0225	0.0275	1.170	24
4	0.0275	0.0225	0.0075	.....	0.0225	0.0225	0.0225	1.178	24
5	0.0325	0.0225	0.0075	.....	0.0075	0.0225	0.0325	1.133	24
6	0.0225	0.0275	0.0225	.....	0.0225	0.0125	0.0225	1.195	22
7	0.0125	0.0225	0.0275	.....	0.0275	0.0225	0.0125	1.221	24
8	0.0225	0.0125	0.0225	.....	0.0225	0.0275	0.0225	1.251	24
9	0.0275	0.0125	0.0125	.....	0.0125	0.0125	0.0275	1.176	23
10	0.0325	0.0125	0.0125	.....	0.0125	0.0125	0.0325	1.173	23
11	0.0125	0.0275	0.0125	.....	0.0125	0.0125	0.0125	1.205	23
12	0.0125	0.0125	0.0275	.....	0.0275	0.0125	0.0125	1.242	24
13	0.0125	0.0125	0.0125	.....	0.0125	0.0275	0.0125	1.207	23

Table 3 The discrete decision information table

No	C_1 $x/c=$-0.5	C_2 -0.4375	C_3 -0.375	....	C_{15} 0.375	C_{16} 0.4375	C_{17} 0.5	D_1 C_{Lmax}	D_2 Stall α
1	1	1	1	.....	1	1	1	2	0
2	3	3	3	.....	3	3	3	1	2
3	3	3	2	.....	2	3	3	1	2
4	3	3	2	.....	2	3	3	1	1
5	3	3	2	.....	2	3	3	1	2
6	3	3	3	.....	3	2	3	1	0
7	2	3	3	.....	3	3	2	2	2
8	3	2	3	.....	3	3	3	3	2
9	3	2	2	.....	2	2	3	1	1
10	3	2	2	.....	2	2	3	1	1
11	2	3	2	.....	2	2	2	2	1
12	2	2	3	.....	3	2	2	3	2
13	2	2	2	.....	2	3	2	2	2

reduction, and these are the three VG installation positions at the top of the model shown in Fig. 1. It indicates that the VG at the wing tip position plays a decisive role in the maximum C_L in the experiment. Furthermore, two rules for the high level of maximum C_L ($D_1=3$) are obtained as follows:

$$R_1 : (C_1, 3; C_2, 2; C_3, 3) \rightarrow (D_1, 3),$$

$$R_2 : (C_1, 2; C_2, 2; C_3, 3) \rightarrow (D_1, 3).$$

Clearly, a high level of maximum lift coefficient requires VG height at the wing tip to change along the spanwise direction.

Next, stall α was taken as the decision attribute for analysis, and only C_1 (x/c = -0.5), C_3 (x/c = -0.375), and C_4 (x/c = -0.3125) were retained after attribute reduction, and these are the three VG installation positions at the top of the model shown in Fig. 1. It indicates that the VG of the wing tip position also plays a decisive role in stall α. Moreover, three rules for the high level of stall α ($D_2 = 3$) are obtained as follows:

$$R_1 : (C_1, 3;\ C_3, 3;\ C_4, 3) \rightarrow (D_2, 3),$$

$$R_2 : (C_1, 2;\ C_3, 3;\ C_4, 3) \rightarrow (D_2, 3),$$

$$R_3 : (C_1, 2;\ C_3, 3;\ C_4, 2) \rightarrow (D_2, 3).$$

Clearly, a high level of stall α requires the VG height at the wing tip to undergo a spanwise change.

The above-mentioned analysis indicates that rough set theory can acquire prior existing knowledge from sample cases and also additional information. In order to improve the maximum C_L and delay stall for the wing, it was necessary to control the wing tip vortex. The above-mentioned rough set analysis results indicate that VGs at the wing tip play a decisive role in the maximum C_L and stall α, which is consistent with the physical evaluations presented in this study.

Moreover, the above-described rough set analysis also indicates that when VG is used to control the wing-tip vortex, in order to achieve a better control effect, VG height should be changed significantly along the spanwise direction in the wing-tip region. Comprehensive analysis of the rules of maximum C_L and stall α indicates that C_1 and C_3 are the conditional attributes (positions) that affect maximum C_L and stall α simultaneously; this information was determined through rough set theory.

Therefore, in order to better control the wing separation flow, the height of the VG needs to be varied along the wingspan direction, in particular, the height of the VG in the wing tip region.

4 Conclusions

In this study, the effect of VG height on the aerodynamic characteristics of an NACA4415 wing was experimentally studied by a wind tunnel experiment, where the VG height distribution was: equal, triangular, and trapezoidal along the wingspan direction, respectively. The research conclusions are as follows:

(1) When the VG height distribution was equal, the maximum C_L decreased to some extent; however, it could inhibit stall flow on the wing. The VG installation density significantly affected its inhibition ability, and "Equal height 17" had an optimal stalling inhibition ability.
(2) When the VG height distribution had a triangular shape, all the stall flow on the wing could be suppressed, and "Triangular shape 1" was better than "Equal height 17". After the translation of "Triangular shape 1", its ability to suppress the wing stall improved further, and "Triangular translation 3" was the best, where the maximum C_L increased by 2.5%, the stall α increased by 2°, and the effective range of α to improve the stall was more than 8°.

(3) When the VG height distribution had a trapezoidal shape, all of the stall flow on the wing could be suppressed, and "Trapezoidal shape 1" was better than "Equal height 17". After the translation of "Trapezoidal shape 1", its ability to suppress the wing stall improved further, and "Trapezoidal translation 2" was the best, where the maximum C_L increased by 1.7%, the stall α increased by 2°, and the effective range of α to improve the stall was more than 8°.
(4) Rough set theory was used to evaluate the control effect of the VG on the stall flow of the wing, and the parameterized analysis of the VG height and position region was also carried out. The results indicated that the variation of the VG height near the wing tip exhibited a significant effect on the development of the wing stall characteristics.

Overall, the control effect with a variable height distribution of VGs was better than that with an equal height distribution, and the change of VG height near the wing tip showed a significant effect on the stall flow control. This study aims to provide technical support for subsequent flow control research based on the height dynamic change of VGs. Undeniably, a lot more systematic explorations are further demanded to study the effect of VG height on the wing tip vortex development, in particular, the dynamic change of the height of VG at the wing tip, and further extend the aforementioned research ideas to the dynamic stall control of the airfoil/wing and flow control around the aircraft, which will be pursued in the future.

Abbreviations

c	Chord
b	Span
C_L	Lift coefficient
C_D	Drag coefficient
Cn	Normal force coefficient
a	Angle of attack
a_0	Zero-lift angle of attack
k	Slope of the normal force line
f	Position of the separation point
h	Height of vortex generator
s	Distance between adjacent vortex generators
n	Number of vortex generators

Acknowledgements
Not applicable.

Authors' contributions
All the authors contributed to and approved this manuscript.

Funding
The present work is supported by the Fundamental Research Funds for the Central Universities (D5050210009).

Availability of data and materials
All data, model, and code that support findings of this study are available from the corresponding author upon reasonable request.

Declarations

Competing interests
The authors declare that they have no competing interests.

Received: 9 October 2022 Accepted: 5 January 2023
Published online: 02 February 2023

References

1. Taylor HD (1947) The elimination of diffuser separation by vortex generator. United Aircraft Corporation Report No. R-4012–3, Wilmington
2. Lin JC (2002) Review of research on low-profile vortex generators to control boundary-layer separation. Prog Aerosp Sci 38(4-5):389–420. https://doi.org/10.1016/S0376-0421(02)00010-6
3. Fernández-Gámiz U, Marika Velte C, Réthoré PE et al (2016) Testing of self-similarity and helical symmetry in vortex generator flow simulations. Wind Energy 19(6):1043–1052. https://doi.org/10.1002/we.1882
4. Lin JC, Robinson SK, McGhee RJ et al (1994) Separation control on high-lift airfoils via micro-vortex generators. J Aircr 31(6):1317–1323. https://doi.org/10.2514/3.46653
5. Joubert G, Le Pape A, Heine B et al (2013) Vortical interactions behind deployable vortex generator for airfoil static stall control. AIAA J 51(1):240–252. https://doi.org/10.2514/1.J051767
6. Saenz-Aguirre A, Fernandez-Gamiz U, Zulueta E et al (2022) Flow control based 5 MW wind turbine enhanced energy production for hydrogen generation cost reduction. Int J Hydrogen Energy 47(11):7049–7061. https://doi.org/10.1016/j.ijhydene.2020.01.022
7. Moon HG, Park S, Ha K et al (2021) CFD-based in-depth investigation of the effects of the shape and layout of a vortex generator on the aerodynamic performance of a multi-MW wind turbine. Appl Sci 11(22):10764. https://doi.org/10.3390/app112210764
8. Lee HM, Kwon OJ (2019) Numerical simulation of horizontal axis wind turbines with vortex generators. Int J Aeronaut Space Sci 20(2):325–334. https://doi.org/10.1007/s42405-018-0118-z
9. Anderson BH, Tinapple J, Surber L (2006) Optimal control of shock wave turbulent boundary layer interactions using micro-array actuation. Paper presented at the 3rd AIAA flow control conference, San Francisco, 5-8 June 2006. https://doi.org/10.2514/6.2006-3197
10. Zhang Y, Tan HJ, Du MC et al (2015) Control of shock/boundary-layer interaction for hypersonic inlets by highly swept microramps. J Propul Power 31(1):133–143. https://doi.org/10.2514/1.B35299
11. Ren SL, Liu PQ (2022) Numerical study on the effect of vortex generators on S-shaped intake in propeller slipstream. J Aerosp Eng 35(3):04022013. https://doi.org/10.1061/(ASCE)AS.1943-5525.0001402
12. Hwangbo H, Ding Y, Eisele O et al (2017) Quantifying the effect of vortex generator installation on wind power production: an academia-industry case study. Renew Energy 113:1589–1597. https://doi.org/10.1016/j.renene.2017.07.009
13. Baldacchino D, Ferreira C, De Tavernier D et al (2018) Experimental parameter study for passive vortex generators on a 30% thick airfoil. Wind Energy 21(9):745–765. https://doi.org/10.1002/we.2191
14. Zhang L, Li XX, Yang K et al (2016) Effects of vortex generators on aerodynamic performance of thick wind turbine airfoils. J Wind Eng Ind Aerodyn 156:84–92. https://doi.org/10.1016/j.jweia.2016.07.013
15. Kim HH, Kim HY, Han JS et al (2018) A development and assessment of variable- incidence angle vortex generator at low Reynolds number of ~5×10^4. Int J Aeronaut Space Sci 19:836–842. https://doi.org/10.1007/s42405-018-0099-y
16. Wang HP, Zhang B, Qiu QG et al (2017) Flow control on the NREL S809 wind turbine airfoil using vortex generators. Energy 118:1210–1221. https://doi.org/10.1016/j.energy.2016.11.003
17. Arunvinthan S, Raatan VS, Pillai SN et al (2021) Aerodynamic characteristics of shark scale-based vortex generators upon symmetrical airfoil. Energies 14(7):1808. https://doi.org/10.3390/en14071808
18. Zhang ZH, Li WW, Jia XN (2020) CFD investigation of a mobula birostris-based bionic vortex generator on mitigating the influence of surface roughness sensitivity of a wind turbine airfoil. IEEE Access 8:223889–223896. https://doi.org/10.1109/ACCESS.2020.3044063
19. Zhu CY, Chen J, Wu JH et al (2019) Dynamic stall control of the wind turbine airfoil via single-row and double-row passive vortex generators. Energy 189:116272. https://doi.org/10.1016/j.energy.2019.116272
20. Zhu CY, Wang TG, Wu JH (2019) Numerical investigation of passive vortex generators on a wind turbine airfoil undergoing pitch oscillations. Energies 12(4):654. https://doi.org/10.3390/en12040654
21. De Tavernier D, Ferreira C, Viré A et al (2021) Controlling dynamic stall using vortex generators on a wind turbine airfoil. Renew Energy 172:1194–1211. https://doi.org/10.1016/j.renene.2021.03.019
22. Le Pape A, Costes M, Richez F et al (2012) Dynamic stall control using deployable leading-edge vortex generators. AIAA J 50(10):2135–2145. https://doi.org/10.2514/1.J051452
23. Troldborg N, Zahle F, Sørensen NN (2016) Simulation of wind turbine rotor with vortex generators. J Phys Conf Ser 753(2):022057. https://doi.org/10.1088/1742-6596/753/2/022057
24. Wu Z, Chen T, Wang H et al (2022) Investigate aerodynamic performance of wind turbine blades with vortex generators at transition area. Wind Eng 46(2):615–629. https://doi.org/10.1177/0309524X211038542
25. Thwaites B (1960) Incompressible Aerodynamics. Clarendon Press, Oxford, New York
26. Wheeler GO (1988) Wind tunnel experimentation on a modified liebeck airfoil. Vortex Internal Report, Sumner
27. Barrett R (1993) An experimental evaluation of smart tetrahedral vortex generators. Dissertation, University of Kansas, Lawrence
28. Barrett R, Farokhi S (1996) Subsonic aerodynamics and performance of a smart vortex generator system. J Aircr 33(2):393–398. https://doi.org/10.2514/3.46950
29. Pawlak Z (1982) Rough sets. Int J Comput Inf Sci 11(5):341–356. https://doi.org/10.1007/BF01001956
30. Chiba K, Oyama A, Obayashi S et al (2007) Multidisciplinary design optimization and data mining for transonic regional-jet wing. J Aircr 44(4):1100–1112. https://doi.org/10.2514/1.17549
31. Chiba K, Jeong S, Obayashi S et al (2006) Knowledge discovery in aerodynamic design space for flyback-booster wing using data mining. Paper presented at the 14th AIAA/AHI space planes and hypersonic systems and technologies conference, Canberra, 6-9 November 2006. https://doi.org/10.2514/6.2006-7992

Publisher's Note